Taylor & Francis
Taylor & Francis Group

ANGIOGRAPHY

Pulmonary vein imaging: comparison of 3D magnetic resonance angiography with 2D cine MRI for characterizing anatomy and size

MUSHABBAR A. SYED,[1] DANA C. PETERS,[1] HAROON RASHID,[2] and ANDREW E. ARAI[1,*]

[1]*Laboratory of Cardiac Energetics, National Heart, Lung and Blood Institute, Department of Health and Human Services, National Institutes of Health, Bethesda, Maryland, USA*
[2]*Division of Cardiology, Georgetown University Hospital, Washington, District of Columbia, USA*

Pulmonary vein imaging is integral for planning atrial fibrillation ablation procedures. We tested the feasibility of quantifying pulmonary vein ostial diameter using two-dimensional cine cardiac magnetic resonance (2D cine CMR) and three-dimensional magnetic resonance angiography (3D MRA). Nine patients with a history of atrial fibrillation and 20 normal volunteers underwent 2D cine CMR and contrast-enhanced 3D MRA of pulmonary veins on a 1.5 T scanner. Pulmonary vein ostial diameters were measured and pulmonary vein vessel border sharpness was graded qualitatively. Both techniques provided excellent pulmonary vein imaging; however, 3D MRA was faster to perform. The average difference between the systolic and diastolic pulmonary vein diameter was 2.5 mm (23.2%, $p < 0.0001$) in normal volunteers and 2.2 mm (16.9%, $p < 0.0001$) in atrial fibrillation patients. The ostial diameter measurements by 3D MRA were significantly larger than on 2D cine CMR. Additionally, the pulmonary vein borders appeared sharper with 2D cine CMR compared to 3D MRA. In conclusion, the 2D images can resolve differences in diameter across the cardiac cycle, while the 3D images provide high quality anatomical depiction but blur borders due to pulsatile motion. We suggest a protocol combining 2D cine CMR and 3D MRA for comprehensive evaluation of pulmonary veins.

Key Words: Pulmonary vein; Magnetic resonance imaging; Magnetic resonance angiography; Atrial fibrillation

1. Introduction

In some patients with atrial fibrillation, the arrhythmia originates in ectopic foci located near the pulmonary veins (1, 2). Most of these ectopic foci (94%) tend to be within 2–4 cm of the junction of the atrium and pulmonary veins, making electrophysiological ablation of these foci possible (1). Pulmonary vein imaging is considered an integral part of this procedure and is currently accomplished by invasive angiography (3), intra-cardiac echocardiography (4, 5), or by computed tomography using iodinated contrast agents (6, 7).

Three-dimensional contrast-enhanced magnetic resonance angiography (3D MRA) is rapidly becoming an important method for the anatomical delineation and sizing of pulmonary veins for pre-ablation planning, and assessment of the patency of pulmonary veins after the ablation procedure (8–12). 3D MRA has the advantage of being noninvasive, does not involve radiation exposure or require iodinated contrast agents, and provides a three-dimensional tomographic evaluation of proximal pulmonary veins with high spatial resolution and excellent contrast. Two-dimensional cine cardiac magnetic resonance (2D cine CMR) imaging of the heart using a segmented ECG-gated steady-state free precession (SSFP) sequence and breath holding is generally considered a reference standard for cardiac and vascular dimensions. This may be important in pulmonary vein imaging since the pulmonary veins, by virtue of their attachment with the heart and the blood pulsatility, move during the cardiac cycle (13, 14).

This study tested the feasibility of using pulmonary vein imaging with ECG-gated 2D cine CMR and contrast-enhanced 3D MRA techniques to delineate anatomy and measure the ostial diameters. We hypothesized that pulsatile motion of the pulmonary veins would blur the vessel borders on the non-ECG gated 3D MRA and would lead to overestimation of the ostial diameters. Therefore, we quantified changes in diameter of the pulmonary veins during systole and diastole using an ECG-gated 2D SSFP technique and compared these measurements with diameters determined from 3D MRA.
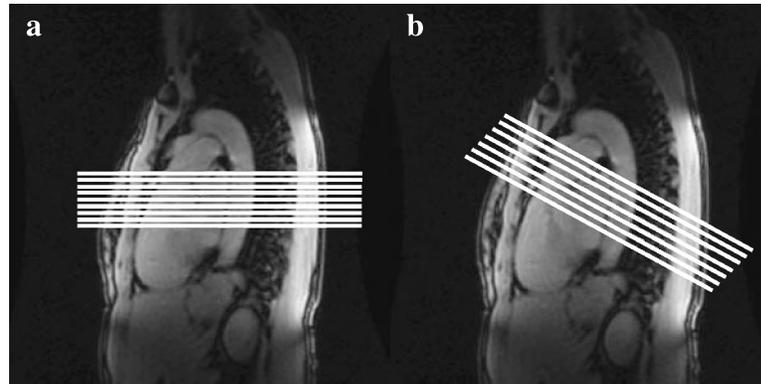
Figure 1. Imaging planes for 2-D cine CMR acquisition. a) axial plane for inferior pulmonary veins. b) oblique plane for superior pulmonary veins.

2. Methods

2.1. *Subjects*

Pulmonary vein MRI imaging was performed on nine patients with atrial fibrillation (AFib), five males, four females, mean age 56.9 ± 6.8 years. Out of these patients, five were in atrial fibrillation at the time of the MRI scan. We also imaged 20 normal volunteers (NV), 10 males, 10 females, mean age 41.7 ± 10.7 years. All patients gave informed consent prior to the study.

2.2. *Pulmonary vein imaging*

All imaging was performed on a 1.5 T MR scanner (Signa CV/*i*, G.E. Medical Systems, WI) using a four-element cardiac phased array coil.

After obtaining scout images, the pulmonary vein imaging protocol began with the 2D cine CMR imaging performed with the following scan parameters: axial and oblique imaging planes, ECG-gating, 12 views per segment, 192×160 matrix, typical field of view 28×28 cm, 5-mm slice

thickness, no gaps, $12-15$ second breath-hold, ± 125 kHz receiver bandwidth, TR/TE/flip = 3.5 ms/1.3 ms/45°. Multiple contiguous slices (roughly six to seven slices) were acquired to cover all the pulmonary veins. With experience we found that an oblique imaging plane parallel to the left ventricular short-axis plane was better for displaying the superior pulmonary veins, whereas the axial plane was better for displaying the inferior pulmonary veins (Fig. 1).

The contrast-enhanced MRA exam was performed using 0.2 mmol/kg of gadolinium-DTPA (Magnevist, Berlex) injected intravenously at 1 cc/s, followed by 20 cc of saline flush at 1 cc/s. Timing the start of the 3D scan was based on a dose-timing scan [2 cc of contrast injected at 1 cc/s, followed by a saline flush (15)]. The start of the scan was timed to begin 4 seconds after first arrival of contrast in the pulmonary veins. Scan parameters were: 3D spoiled gradient echo acquisition, coronal plane, 256×192 matrix with three-fourths phase field of view, $2-3$-mm thick slices (zero-filled to $1-1.5$-mm thickness), $24-16$ partitions, ± 32 kHz receiver bandwidth, TR/TE/flip = 5 ms/1.5 ms/45°, fractional echo, and a sequential acquisition order.
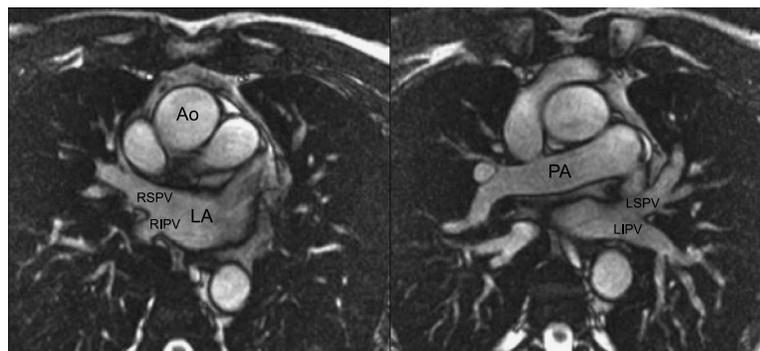

Figure 2. 2D cine CMR images of the pulmonary veins in a normal volunteer. Abbreviations: PA = pulmonary artery, Ao = aorta, LA = left atrium, LSPV = left superior pulmonary vein, RSPV = right superior pulmonary vein, LIPV = left inferior pulmonary vein, RIPV = right inferior pulmonary vein.
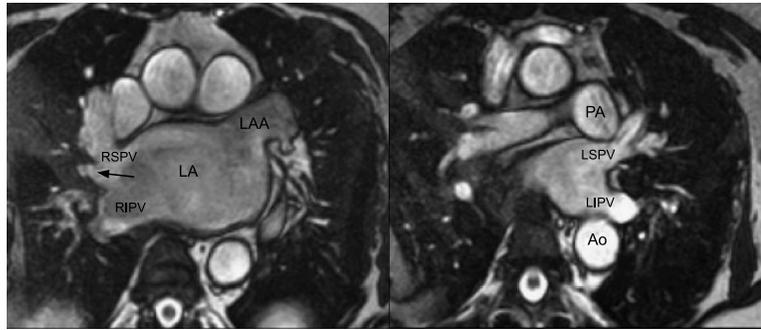
Figure 3. 2D cine CMR images of pulmonary veins in a patient with atrial fibrillation. The arrow points to the right accessory pulmonary vein.

2.3. *Pulmonary vein measurements*

On 2D cine CMR images, the largest (i.e., in systole) and smallest (i.e., in diastole) pulmonary vein cross-sectional diameters across the cardiac cycle were identified and the measurements were made at the ostium (veno-atrial junction). The 3D data sets were reformatted on the scanner console (General Electric Medical Systems) to view the pulmonary veins in cross-section for ostial measurements.

2.4. *Pulmonary vein border sharpness (sharpness score)*

To qualitatively assess the pulmonary vein border sharpness, we devised a Sharpness Score as follows: 1 = poor, 2 = fair, 3 = good, and 4 = excellent border sharpness. Each pulmonary vein was then assigned a Sharpness Score on 2D cine CMR and 3D MRA images.

2.5. *Statistical analysis*

All measures are reported as mean ± standard deviation. The 2D SSFP and 3D MRA measurements were compared using the Student's t-test. The cut-off for statistical significance was $p < 0.05$.

3. Results

Pulmonary vein imaging by 2D cine CMR was successfully completed in all 29 subjects, while one normal volunteer had an unsuccessful 3D MRA due to a contrast injection error.

3.1. *Pulmonary vein anatomy*

Anatomical classification was based on the description by Kato et al. (10). Pulmonary vein anatomy by 2D cine CMR and 3D MRA imaging is shown in Figs. 2–5. Most of the subjects (66%) had the typical anatomy with four pulmonary vein ostia (Fig. 2: 13 normal volunteers and six atrial fibrillation patients). The next common pattern was an accessory right pulmonary vein from the middle lobe (28%, Figs. 3 and 4: five normal volunteers, three atrial fibrillation patients), followed by a short common left trunk (14%, Fig. 5a: four normal volunteers), combined right accessory vein and short common left trunk (10%, three normal volunteers), and a long common left trunk (3%, Fig. 5b: one normal volunteer). Atrial fibrillation did not adversely affect pulmonary vein image quality for either 2D or 3D acquisitions.
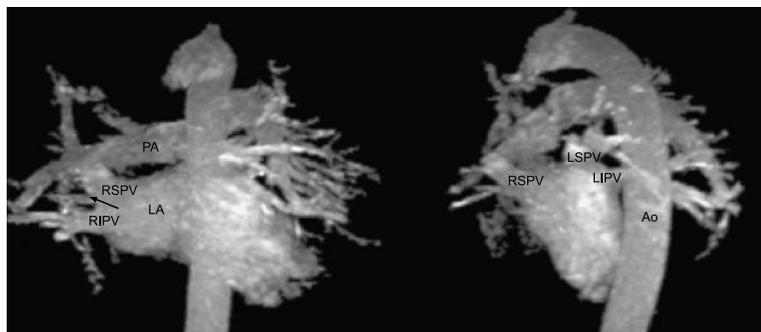

Figure 4. 3D MRA of pulmonary veins. Right accessory pulmonary vein is shown (arrow). Abbreviations as in prior figures.
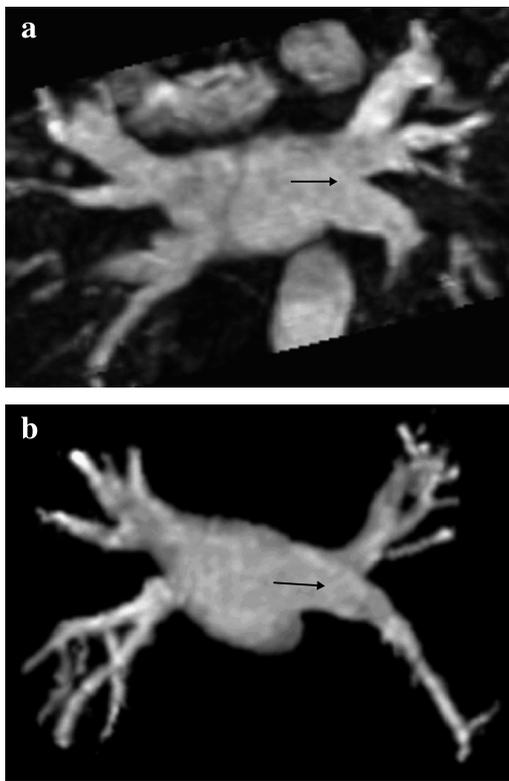
Figure 5. Pulmonary vein anatomical variants. a) Short left common trunk (arrow). b) Long left common trunk (arrow).

3.2. *Pulmonary vein size*

Pulmonary vein diameter measurements by 2D cine CMR are summarized in Table 1. In normal volunteers, the left inferior pulmonary vein had the smallest diameter compared to other pulmonary veins. For all pulmonary veins there was a significant difference between the largest and the smallest pulmonary vein diameter across the cardiac cycle, with an average difference of 2.5 mm ($p < 0.0001$).

In patients with atrial fibrillation, the inferior pulmonary vein also had the smallest diameter. The average difference
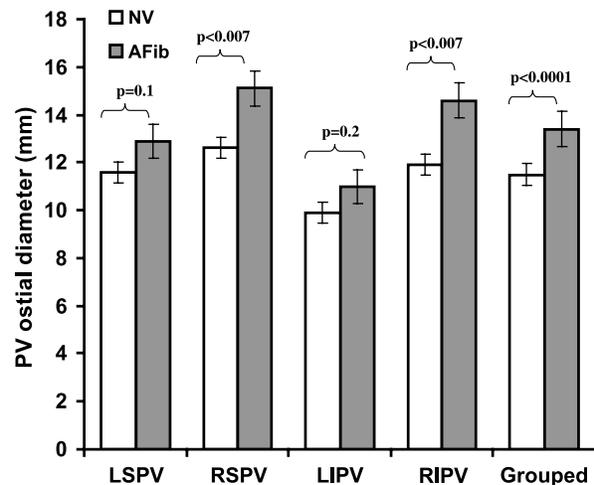

Figure 6. Pulmonary vein ostial diameter in normal volunteers compared to patients with atrial fibrillation.

between the largest and smallest diameter across the cardiac cycle was 2.2 mm ($p < 0.0001$). Overall, the mean diameter change was less in patients with atrial fibrillation compared to normal volunteers ($p = 0.03$).

Figure 6 displays the pulmonary vein diameter comparison between patients with atrial fibrillation and normal volunteers. When all pulmonary veins were grouped together, the pulmonary vein diameters were larger in patients with atrial fibrillation compared with normal volunteers ($p < 0.0001$). For individual veins, the right superior and inferior pulmonary veins were significantly larger in patients with atrial fibrillation, while the left superior and inferior veins were not significantly different between the two groups.

Table 2 compares the 3D MRA measurements with the 2D cine CMR in normal volunteers and patients with atrial fibrillation. Overall, the ostial diameters by 3D MRA were significantly larger than 2D cine CMR measurements, both in normal volunteers ($p < 0.0001$) and in patients with atrial fibrillation ($p = 0.005$).

Table 1. Pulmonary vein ostial measurements by 2-D cine CMR

Measured site	LSPV (mm)	RSPV (mm)	LIPV (mm)	RIPV (mm)	Grouped (mm)
NV					
Largest	13.2 ± 1.9	14.0 ± 1.8	10.9 ± 1.6	13.0 ± 2.3	12.8 ± 2.2
Smallest	10.4 ± 2.2	11.1 ± 1.9	8.8 ± 1.7	10.9 ± 2.0	10.9 ± 2.1
Difference	2.9 ± 1.4	2.9 ± 1.9	2.2 ± 1.1	2.2 ± 1.6	2.5 ± 1.6
p-value	< 0.0001	< 0.0001	< 0.0001	< 0.0001	< 0.0001
AFib					
Largest	13.5 ± 2.6	16.5 ± 3.3	11.9 ± 2.3	16.1 ± 3.6	14.5 ± 3.5
Smallest	12.4 ± 2.8	13.6 ± 2.7	10.0 ± 2.6	13.2 ± 2.7	12.3 ± 2.9
Difference	1.1 ± 1.3	2.8 ± 1.6	1.9 ± 1.8	3.0 ± 1.7	2.2 ± 1.7
p-value	0.03	0.001	0.01	0.001	< 0.0001

Table 2. 2-D cine CMR vs. 3-D MRA pulmonary vein measurements

Imaging technique	LSPV (mm)	RSPV (mm)	LIPV (mm)	RIPV (mm)	Grouped (mm)
NV					
2D mean	11.6 ± 2.0	12.6 ± 1.6	9.9 ± 1.6	11.9 ± 2.0	11.5 ± 2.0
3D	13.7 ± 1.5	13.3 ± 2.5	12.9 ± 2.4	13.8 ± 2.1	13.4 ± 2.2
p-value	0.005	0.16	< 0.0001	0.006	< 0.0001
AFib					
2D mean	12.9 ± 2.6	15.1 ± 2.9	11.0 ± 2.3	14.6 ± 3.1	13.4 ± 3.1
3D	14.2 ± 1.6	16.1 ± 2.5	14.1 ± 4.1	14.5 ± 2.0	14.7 ± 2.7
p-value	0.07	0.13	0.02	0.83	0.005

3.3. *Sharpness score and pulmonary vein motion*

Table 3 displays the sharpness score for all pulmonary veins in normal volunteers and in atrial fibrillation patients. In both groups, the pulmonary vein borders appeared more blurred with the 3D MRA technique as characterized by significantly lower sharpness scores compared to 2D cine CMR technique.

4. Discussion

We compared pulmonary vein imaging by ECG-gated 2D cine CMR technique with a non-ECG-gated 3D MRA method. The size of pulmonary veins was overestimated by 3D MRA measurements compared to 2D cine CMR. Pulmonary vein size changes significantly in systole and diastole as measured by 2D cine CMR. The pulmonary vein borders were significantly more blurred on the 3D MRA acquisition than 2D cine CMR. We believe this blurring is due to the pulmonary vein pulsatile motion and displacement across the cardiac cycle leading to overestimation of pulmonary vein size with a non-ECG-gated MRA.

Interestingly, in patients with atrial fibrillation, the significant difference between 3D and 2D measurements was not seen in all pulmonary veins, which may be due to decreased pulmonary vein pulsatility in atrial fibrillation. We also found that the right-sided pulmonary veins were larger in patients with atrial fibrillation than in normal volunteers.

Table 3. Sharpness score

Imaging technique	LSPV	RSPV	LIPV	RIPV
NV				
2D	3.2 ± 0.6	3.5 ± 0.7	3.7 ± 0.6	3.5 ± 0.9
3D	2.2 ± 0.8	2.0 ± 0.7	2.2 ± 0.7	2.7 ± 0.5
p-value	0.0003	< 0.0001	< 0.0001	0.001
AFib				
2D	3.4 ± 0.7	3.6 ± 0.5	3.7 ± 0.5	3.4 ± 0.7
3D	2.3 ± 0.5	2.3 ± 0.7	2.1 ± 0.6	2.2 ± 0.4
p-value	0.01	0.005	0.001	0.002

Note: Sharpness score: 1 = poor, 2 = fair, 3 = good, 4 = excellent.

The most common anatomical variant in our study was the presence of a right accessory pulmonary vein. This was followed by the presence of common trunk, mostly on the left side. Anatomical definition of the pulmonary veins and their variants was roughly equivalent using 2D cine CMR and 3D MRA.

Because of the emergence of atrial fibrillation ablation therapy, there is great interest in characterizing the anatomy and size of pulmonary veins to provide a "road map" for the procedure and to monitor for post-procedure pulmonary vein stenosis. Increasingly, electroanatomical mapping systems allow incorporation of CMR data to construct cardiac anatomy during the electrophysiological procedure. There are several reports in the literature, all of which have exclusively used 3D MRA techniques for this purpose. In patients with atrial fibrillation, Wittkampf et al. (9) found that the pulmonary vein ostial diameter varied significantly depending upon the projection used for measurement. This difference was more pronounced in left-sided pulmonary veins based on their oval shaped ostia compared to more round shaped ostia of the right sided pulmonary veins. Kato et al. (10) also found the pulmonary vein ostia to be oblong with the superior-inferior diameter significantly greater than the anterior-posterior diameter, but did not find significant differences in pulmonary vein diameters within a given patient. However, both studies used non-ECG-gated 3D MRA techniques for image acquisition and did not compare this with ECG-gated 2D cine CMR. Our study demonstrates that because of pulmonary vein motion across the cardiac cycle and non-gated acquisition, the 3D MRA overestimates the pulmonary vein diameter.

4.1. *Limitations*

The study has several limitations that must be considered. The 3D data sets were collected with 1.5-mm-thick slices (zero filled), which was lower than the in-plane resolution, thereby perhaps contributing to spatial blur. However, this slice-thickness (2–3 mm) is typical of that used in pulmonary vein assessment with contrast MRA (16–18). Since the pulmonary veins are attached to the cardiac chamber, the 3D data may also be blurred by translational motion during the cardiac cycle, which we did not measure. The pulmonary vein

measurements were made in the anterior-posterior plane, which may provide slightly smaller diameter than the superior-inferior plane measurements; however, as both 2D cine CMR and 3D MRA measurements were done in the same plane, this is unlikely to affect the results of this study. Although 2D cine CMR provided excellent pulmonary vein imaging for measurements, it required a breath hold for acquiring each slice (usually six to eight slices to cover all pulmonary veins). On the other hand, 3D MRA required only two breath holds (20–25 seconds each), was faster to perform, and provided excellent anatomical information.

5. Conclusion

Pulmonary vein imaging with the 2D cine CMR using ECG-gated steady-state free precession technique provides easily measurable largest and smallest ostial diameters across the cardiac cycle. This technique is useful for pulmonary vein imaging in patients with atrial fibrillation as well as sinus rhythm. Pulmonary veins ostial diameter change significantly between systole and diastole, around 2–2.5 mm (17%–24%) in atrial fibrillation patients and normal volunteers, which contributes to blurring of pulmonary vein borders. These findings may be useful when imaging pulmonary veins and sizing vein ostia for ablation procedures. We suggest a protocol combining 2D cine CMR and 3D MRA for comprehensive evaluation of pulmonary veins in clinical practice. The 2D images are sharper and can resolve differences in diameter across the cardiac cycle, while the 3D images provide high quality anatomical depiction but blur borders due to pulsatile motion.

Abbreviations

SSFP	steady-state free precession
2D	two-dimensional
3D MRA	three-dimensional magnetic resonance angiography
NV	normal volunteer
AFib	atrial fibrillation
LSPV	left superior pulmonary vein
LIPV	left inferior pulmonary vein
RSPV	right superior pulmonary vein
RIPV	right inferior pulmonary vein

References

1. Haissaguerre M, Jais P, Shah DC, Takahashi A, Hocini M, Quiniou G, Garrigue S, Le Mouroux A, Le Metayer P, Clemety J. Spontaneous initiation of atrial fibrillation by ectopic beats originating in the pulmonary veins. N Engl J Med 1998; 339:659–666.
2. Chen SA, Hsieh MH, Tai CT, Tsai CF, Prakash VS, Yu WC, Hsu TL, Ding YA, Chang MS. Initiation of atrial fibrillation by ectopic beats originating from the pulmonary veins: electrophysiological characteristics, pharmacological responses, and effects of radiofrequency ablation. Circulation 1999; 100:1879–1886.
3. Oral H, Scharf C, Chugh A, Hall B, Cheung P, Good E, Veerareddy S, Pelosi F Jr, Morady F. Catheter ablation for paroxysmal atrial fibrillation: segmental pulmonary vein ostial ablation versus left atrial ablation. Circulation 2003; 108:2355–2360.
4. Marrouche NF, Martin DO, Wazni O, Gillinov AM, Klein A, Bhargava M, Saad E, Bash D, Yamada H, Jaber W, Schweikert R, Tchou P, Abdul-Karim A, Saliba W, Natale A. Phased-array intracardiac echocardiography monitoring during pulmonary vein isolation in patients with atrial fibrillation: impact on outcome and complications. Circulation 2003; 107:2710–2716.
5. Donal E, Grimm RA, Yamada H, Kim YJ, Marrouche N, Natale A, Thomas JD. Recovery of left atrial function following pulmonary vein isolation using radiofrequency ablation in chronic atrial fibrillation: an intracardiac doppler echocardiographic study. J Am Coll Cardiol 2003; 4:448–449.
6. Perez-Lugones A, Schvartzman PR, Schweikert R, Tchou PJ, Saliba W, Marrouche NF, Castle LW, White RD, Natale A. Three-dimensional reconstruction of pulmonary veins in patients with atrial fibrillation and controls: morphological characteristics of different veins. Pacing Clin Electrophysiol 2003; 26:8–15.
7. Qureshi AM, Prieto LR, Latson LA, Lane GK, Mesia CI, Radvansky P, White RD, Marrouche NF, Saad EB, Bash DL, Natale A, Rhodes JF. Transcatheter angioplasty for acquired pulmonary vein stenosis after radiofrequency ablation. Circulation 2003; 108:1336–1342.
8. Dill T, Neumann T, Ekinci O, Breidenbach C, John A, Erdogan A, Bachmann G, Hamm CW, Pitschner HF. Pulmonary vein diameter reduction after radiofrequency catheter ablation for paroxysmal atrial fibrillation evaluated by contrast-enhanced three-dimensional magnetic resonance imaging. Circulation 2003; 107:845–850.
9. Wittkampf FH, Vonken EJ, Derksen R, Loh P, Velthuis B, Wever EF, Boersma LV, Rensing BJ, Cramer MJ. Pulmonary vein ostium geometry: analysis by magnetic resonance angiography. Circulation 2003; 107:21–23.
10. Kato R, Lickfett L, Meininger G, Dickfeld T, Wu R, Juang G, Angkeow P, LaCorte J, Bluemke D, Berger R, Halperin HR, Calkins H. Pulmonary vein anatomy in patients undergoing catheter ablation of atrial fibrillation: lessons learned by use of magnetic resonance imaging. Circulation 2003; 107:2004–2010.
11. Tsao HM, Yu WC, Cheng HC, Wu MH, Tai CT, Lin WS, Ding YA, Chang MS, Chen SA. Pulmonary vein dilation in patients with atrial fibrillation: detection by magnetic resonance imaging. J Cardiovasc Electrophysiol 2001; 12:809–813.
12. Vonken EPA, Velthuis BK, Wittkampf FH, Rensing BJ, Dersken R, Cramer MJM. Contrast enhanced MRA and 3D visualization of pulmonary venous anatomy to assist radiofrequency catheter ablation. J Cardiovasc Magn Res 2003; 5:545–551.
13. Foo TK, MacFall JR, Hayes CE, Sostman HD, Slayman BE. Pulmonary vasculature: single breath-hold MR imaging with phased-array coils. Radiology 1992; 183:473–477.
14. Link KM, Loehr SP, Lesko NM. Cardiopulmonary vascular imaging. Invest Radiol 1992; 27(Suppl. 2):S72–S79.
15. Earls JP, Rofsky NM, DeCorato DR, Krinsky GA, Weinreb JC. Breath-hold single-dose gadolinium-enhanced three-dimensional MR aortography: usefulness of a timing examination and MR power injector. Radiology 1996; 201:705–710.
16. Stein PD, Woodard PK, Hull RD, Kayali F, Weg JG, Olson RE, Fowler SE. Gadolinium-enhanced magnetic resonance angiography for detection of acute pulmonary embolism: an in-depth review. Chest 2003; 124:2324–2328.
17. Oudkerk M, van Beek EJ, Wielopolski P, van Ooijen PM, Brouwers-Kuyper EM, Bongaerts AH, Berghout A. Comparison of contrast-enhanced magnetic resonance angiography and conventional pulmonary angiography for the diagnosis of pulmonary embolism: a prospective study. Lancet 2002; 359:1643–1647.
18. Kauczor H-U. Contrast-enhanced magnetic resonance angiography of the pulmonary vasculature: a review. Invest Radiol 1998; 33:606–617.